



HAL
open science

Relationship between cohesion, processability and bending behavior of carbon rovings

Audrey Hivet, Anwar Shanwan, Samir Allaoui, Gilles Hivet, Romain Nunez

► **To cite this version:**

Audrey Hivet, Anwar Shanwan, Samir Allaoui, Gilles Hivet, Romain Nunez. Relationship between cohesion, processability and bending behavior of carbon rovings. *Journal of Industrial Textiles*, 2024, 54, 10.1177/15280837241261898 . hal-04811458

HAL Id: hal-04811458

<https://hal.univ-reims.fr/hal-04811458v1>

Submitted on 6 Dec 2024

HAL is a multi-disciplinary open access archive for the deposit and dissemination of scientific research documents, whether they are published or not. The documents may come from teaching and research institutions in France or abroad, or from public or private research centers.

L'archive ouverte pluridisciplinaire **HAL**, est destinée au dépôt et à la diffusion de documents scientifiques de niveau recherche, publiés ou non, émanant des établissements d'enseignement et de recherche français ou étrangers, des laboratoires publics ou privés.



Distributed under a Creative Commons Attribution - NonCommercial 4.0 International License

Relationship between cohesion, processability and bending behavior of carbon rovings

Volume 54: 1–24

© The Author(s) 2024

Article reuse guidelines:

sagepub.com/journals-permissions

DOI: 10.1177/15280837241261898

journals.sagepub.com/home/jit

Audrey Hivet¹ , Anwar Shanwan¹ , Samir Allaoui² ,
Gilles Hivet¹ and Romain Nunez³

Abstract

Many manufacturing processes of fibrous composites involve fiber movement to obtain a targeted fibrous preform before the resin is injected or polymerized. The ability of the fibers to move within the yarn can be named “cohesion.” To obtain a correct preform, it is of great importance to know and master yarn cohesion. As there is currently no available method to characterize yarn cohesion upstream, the process parameters have very often to be tuned using lengthy trial and error strategies. This paper proposes to address this issue, demonstrating that the yarn cantilever bending test is a very promising and efficient candidate to characterize and quantify yarn cohesion. In addition, the test can be easily performed in an industrial context and is sensitive enough to discriminate small variations in cohesion, even small discrepancies resulting from the yarn manufacturing process. Above all, thanks to real manufacturing tests on different yarns, this paper shows that the upstream identification of cohesion using the proposed cantilever bending test achieves the goal of predicting the yarn processability.

¹Laboratoire de Mécanique Gabriel Lamé, Université d'Orléans, Orléans, France

²Institut de Thermique, Mécanique, Matériaux EA 7548, University of Reims Champagne-Ardenne, Charleville-Mézières 08000, France

³Safran Ceramics, Safran, Le Haillan, France

Corresponding author:

Audrey Hivet, Laboratoire de Mécanique Gabriel Lamé, Université d'Orléans, 8 rue Léonard de Vinci, Orléans 45100, France.

Email: audrey.hivet@univ-orleans.fr



Creative Commons Non Commercial CC BY-NC: This article is distributed under the terms of the Creative Commons Attribution-NonCommercial 4.0 License (<https://creativecommons.org/licenses/by-nc/4.0/>) which permits non-commercial use,

reproduction and distribution of the work without further permission provided the original work is attributed as specified on the SAGE and Open Access pages (<https://us.sagepub.com/en-us/nam/open-access-at-sage>).

Keywords

Technical yarns, fibrous materials, carbon fibers, processing, cohesion, bending test

Introduction

Carbon yarns are widely used in several industrial applications, especially in the aeronautical and space industries. In structural parts, composites with long quasi parallel fibers are usually used for their interesting mechanical properties. The fibers are initially organized in yarns or tows and then assembled to obtain woven fabrics, nonwoven fabrics, or stitching fabrics. To obtain composite parts, different manufacturing processes can be used during which the fibrous microstructure that forms the yarn is modified. It can be slightly modified, for example, by simple compaction leading to an increase in the fiber volume fraction, or it can be strongly impacted by fiber transfers during processes such as tufting, cracking, needlepunching, yarn placement, etc. In all cases, it is the fibers' ability to move relative to each other which is highlighted. This property can be named the "cohesion" of a fibrous network. Many manufacturers observe that this property has a significant impact on the smooth running and the result of the manufacturing process. At the macroscale, that is the cohesion of woven or stitched fabrics, numerous studies can be found in the literature¹⁻⁷ but with different approaches from the one presented here. Likewise, the cohesion between fibers and matrix has also already been studied.⁸

However, although the intra-yarn cohesion is fundamental for some manufacturing processes which directly involve fiber mobility, to our knowledge, only a few publications^{9,10} have studied this problem. While some studies have been conducted on twisted yarns,¹¹⁻¹⁴ none concern the untwisted yarns considered in this study. Our previous study¹⁵ focused on this question and demonstrated the relation between "processability," that is the smooth running of the manufacturing process, and cohesion. It is therefore crucial to be able to characterize this property finely and reliably to allow the manufacturer to anticipate that the process will proceed with optimal settings and without a long and expensive tuning campaign. Nowadays, the most common method used is tuning by trial and error campaigns, correcting the parameters empirically. Currently, therefore, there is no way to predict the process results before testing in the real industrial application. The present study enables two major industrial problems to be overcome:

- firstly, it demonstrates that yarn cohesion is the parameter that drives the process results. This makes it possible to propose a material property that anticipates the process behavior and hence the results.
- secondly, and most importantly, the present study proposes a very simple and sensitive test to characterize yarn cohesion: yarn bending. This test can be very easily used, even within the production zone, to perform material incoming inspection before the yarn is processed. The test can also be used in the lab in order to source new materials, structures, etc.

To better master processes, however, it is first necessary to consider the relation between cohesion and mechanical properties.

A yarn or a fabric is by definition a fibrous structure. Its mechanical behavior results from the behavior of the constitutive fibers and also from their tangling and interactions. Several mechanical tests are strongly influenced by cohesion and can be used to highlight it. Among them, a potential candidate is the shear test, which directly involves fiber sliding. A previous study¹⁵ showed the ability of the shear test to reliably characterize cohesion but also the numerous drawbacks of this strategy, particularly the great difficulty of conducting the tests, especially for broad yarns; another drawback is the great variability of the results, requiring a large number of tests to converge to a consistent average. Thus, it would be useful to propose another strategy.

A possible alternative would be to resort to a fiber/fiber or yarn/yarn friction test, but these tests do not reveal the influence of the internal microstructure. Another alternative is to resort to a bending test. This test is simple to perform and exhibits at first order the cohesion in the longitudinal direction of the fibrous network. In a multiply or multifiber structure, the bending behavior results from two parameters: the first one is the bending behavior of the constituents (layers, fibers); the second one is the cohesion between layers or fibers. This can be illustrated with a simplified two-dimensional diagram of a rectangular section beam (Figure 1). If the assembly is composed of parallel layers or fibers, not linked to each other, the bending behavior of the whole is equivalent to the bending behavior of the components; in this case the straight section remains in the initial plane (Figure 1(a)). Contrarily, if the layers are completely linked, without any possible mobility, the mechanical behavior is, in a first approximation, that of the equivalent homogeneous structure (Figure 1(b)).

If there is no interaction between the fibers, the bending stiffness of fibrous media is framed by the bending behavior of the fibers; this is defined as no yarn cohesion. If no movements are possible between the fibers, the bending stiffness is framed by the equivalent homogeneous material. The difference between these two cases is considerable, particularly when the fibers are numerous. Consequently, the yarn stiffness value depends on the ability of the fiber to move and slide within the fibers, which is, in this

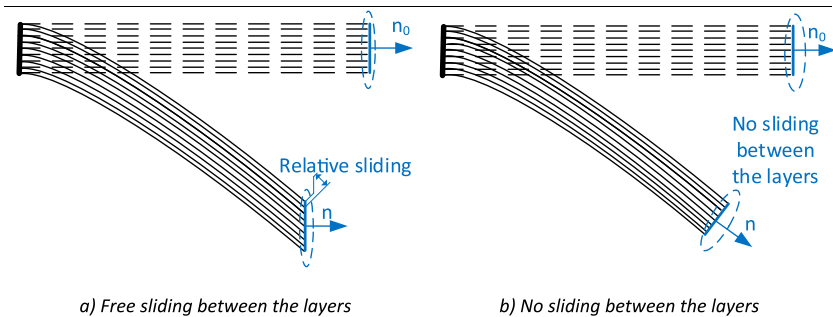


Figure 1. Simplified scheme of a multilayer bending assembly. (a) Free sliding between the layers. (b) No sliding between the layers.

paper, defined as the yarn cohesion. This intuitively simple principle makes the bending test an interesting candidate to highlight the cohesion of a fibrous network. This point will be developed in the following section.

Potential of the bending test to characterize yarn cohesion

To ascertain the interest of the bending test, it is first necessary to evaluate the sensitivity of the relation between cohesion and bending behavior. This can be achieved by studying the bending stiffness ratio between the extreme cases (fibers completely linked and fibers without any interaction) on a simple example of a regular rectangular stacking (Figure 2). As this is merely an introductory calculation intended to show the potential of the method, it can be done within the context of infinitesimal strain theory. The ratio between the quadratic moment of the fiber $I_{G_{ix}}(f_i)$ (fibers without any interaction) and that of the solid equivalent to the set of fibers $I_{Ox}(ya)$ (fibers totally linked) is fully calculated in Appendix 1 and the result is given by equation (1).

$$\frac{I_{Ox}(ya)}{I_{G_{ix}}(f_i)} = n + \frac{16}{3}n_b k_h (k_h + 1)(2k_h + 1) \quad (1)$$

with n , the number of lines of fibers, n_b , the number of fibers in a line and k_h given by $n = 2k_h + 1$.

The yarn is embedded on the one hand, and, on the other hand, it bends under its own weight. In the case of totally independent fibers, an approximation of the curvature is given by:

$$c_{f_i} = \frac{M_{f_i}}{E_f I_{G_{ix}}(f_i)} \quad (2)$$

and of the overhanging length by:

$$y_{Mi} = \frac{p_i l_f^4}{8E_f I_{G_{ix}}} \quad (3)$$

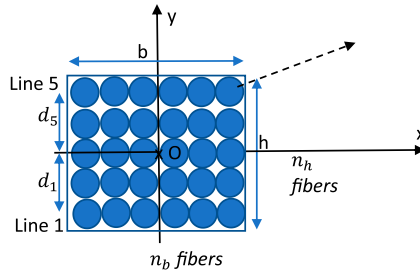


Figure 2. Example of a rectangular fiber bundle.

with $p_i = \frac{\rho_f \pi d_f^2}{4}$

In the case of totally linked fibers, the yarn curvature and overhanging length can be expressed by:

$$c_{ya} = \frac{M_{fya}}{E_f I_{Ox}(ya)} \quad (4)$$

$$y_{M_{ya}} = \frac{p_{ya} l_f^4}{8 E_f I_{Gix}} \quad (5)$$

But in this case, the load linear density includes the number of fibers, then:

$$M_{fya} = n M_{fi} \quad (6)$$

$$p_{ya} = n p_i \quad (7)$$

And the curvature or overhanging length ratio is:

$$\frac{c_{ya}}{c_{fi}} = \frac{y_{M_{ya}}}{y_{M_{fi}}} = 1 + \frac{16}{3n} n_b k_h (k_h + 1) (2k_h + 1) \quad (8)$$

with $n = n_b (2k_h + 1)$

$$\frac{c_{ya}}{c_{fi}} = \frac{y_{M_{ya}}}{y_{M_{fi}}} = 1 + \frac{16}{3} k_h (k_h + 1) \quad (9)$$

The ratio between the quadratic moment of a set of totally consistent fibers (no possible mobility) and a set of free fibers increases quadratically with the number of fibers in the thickness of the yarn. Moreover, depending on the cohesion of the fiber network, the bending stiffness may vary between the two extreme behaviors defined by the two quadratic moments expressed above.

Thus, the greater the number of fibers, the more sensitive the bending stiffness is to cohesion. In the case of fiber yarns, the number of fibers is often in the order of several thousand (50k for most of the yarns presented here). This is therefore a very favorable case to link bending stiffness and cohesion and that is what will be experimentally demonstrated in this study. For example, considering a theoretical yarn close to those studied here, the above equations give:

$$n = 50000, d_f = 6 \mu\text{m}, \frac{2n_b}{n_b} = \frac{1}{9}$$

$$n_b = 3\sqrt{n} \approx 671$$

$$n_h = \frac{\sqrt{n}}{6} \approx 37$$

$$\frac{c_{ya}}{c_{fi}} = \frac{y_{M_{ya}}}{y_{M_{fi}}} = 7500$$

Obviously, this is an ideal case, and the cohesion can never reach these theoretical extrema; however, this calculation illustrates the strong link between bending and cohesion.

When the components are neither totally free nor totally linked, the bending behavior is in between these two extrema. Moreover, the greater the number of subsets, the more distant the extreme behaviors are and the more sensitive the bending stiffness is to cohesion. This is typically the case for long fiber yarns or nonwoven fabrics where:

- Yarns are composed of a high number of fibers in both section directions, especially for the yarns studied here (50k fibers).
- Fibers are neither free nor totally united; this is all the truer with a low average sizing rate.

The cohesion between fibers depends on numerous parameters among which: fiber section (shape, surface condition), tangle, sizing, fiber material, etc. The aim of this study is not to focus on the origin of the cohesion but to analyze the bilateral relation between cohesion and yarn mechanical behavior. The goal is twofold: on the one hand, to find a way to characterize cohesion and on the other hand, to understand some specificities of the yarn mechanical behavior in terms of cohesion.

In conclusion, the bending stiffness appears to be a good candidate to account for and characterize yarn cohesion. The aim of the present study is to confirm this potential and highlight the few drawbacks of this type of test.

Material and methods

Material

To carry out this study, seven batches of yarns, of different types and compositions, were used to characterize cohesion. As mentioned above, all the studied yarns are made with quasi-parallel fibers and will be called roving yarns or rovings in this article. The yarns were chosen to illustrate two main goals: the first one is to be able to illustrate the ability of the strategy to perform material incoming inspection, predicting the process behavior for a given batch without a lengthy trial and error procedure, even with slight changes in the sizing rate. The second one is to be able to source other materials (fibers, structures, etc.). In that case, since many different types of yarns and fibers exist, it is all the more important to have a simple test that can be applied to select the few of them that might be usable without having to undertake the manufacturing process.

In the present study, each batch of roving yarns was assigned an alphabetical letter: A, B, C, D, E, F and G. The seven batches are made of two different types of roving yarns. In yarns F and G, the fibers are smooth, straight, and have less tangling and tortuosity than the other rovings. Roving F is of aeronautical quality (high quality) whereas roving G is of intermediate quality. The second group comprises the roving yarns of the other batches A, B, C, D, E, that have an industrial quality, that is a rougher and more irregular surface and more tangling and tortuosity than roving yarns F and G. The fibers of the different batches

underwent a sizing process using different rates of two sizing materials (Table 1): an epoxy for roving yarns A and F and an antistatic sizing in the other batches (B, C, D, E, and G).

For confidential reasons, the composition and the characteristics of these roving yarns have been replaced by normalized values, as presented in Table 1. It must be mentioned that the sizing ratio is very small with very low variations especially for batches B, C, E. The roving's processability, that is, the ability of a roving yarn to be formed with the considered process, is represented by a cohesion factor (inverse to the processability) between 0 and 3 where 3 means a high cohesion and a more difficult processability and 0 a low cohesion and an easier and more efficient processability. This classification was defined by the manufacturer as a function of the quality of the obtained part and the time needed to tune the process when using these materials.

Observation and analysis made it possible to establish that roving yarn cohesion, that is, the ability of fibers to move relative to each other, can be the origin of the differences in behavior during the forming process. The processes used involve the mobility of fibers (sliding, transfer, etc.) to a significant extent. Some complex and crucial problems then arise:

- As there is some variability between material batches, how can an efficient material incoming inspection be implemented to ensure the smooth running of the process? Slight variations in the average sizing rate can lead to notable differences during the process; that is why several batches of the same material with different sizing rates (B, C, D, E) were compared here.
- How should a change in sizing type (batch A) or fiber type (batches F and G) be made, without implementing a long and uncertain test campaign?
- More generally, defining and intrinsically measuring the cohesion of fibrous reinforcements is still an issue whereas it is crucial for their mechanical behavior; this should be all the more useful in the case of roving yarns with different structures.

To answer this threefold issue, it is essential to have a simple, fast and reliable test for the determination of roving yarn cohesion. The preliminary study above indicated that the bending test may be the answer. Thus, the question is: does a bending test determine with sufficient accuracy the cohesion between different roving yarns, making it possible to anticipate their processability? In other words, does this test enable an intrinsic measure of fabric cohesion to be determined?

Experimental method

Characterizing textile bending behavior has been the subject of study and development for several decades. Peirce was one of the first to study the bending properties of textiles¹⁶ by developing an approach which assumes that the bending moment has a linear dependence on the curvature and in which bending stiffness is calculated at a single deflection position. This approach has been used by several studies^{17–19} and improved by adopting a vertical position of the fabric in order to overcome the effect of sample twist.^{20–22} Other

Table 1. Yarns' characteristics.

	Batch A	Batch B	Batch C	Batch D	Batch E	Batch F	Batch G
Mass per unit length (g.m^{-1})	2.86	2.98	3.04	2.99	2.67	0.60	2.53
Sizing type	Epoxy 1	Antistatic	Antistatic	Antistatic	Antistatic	Epoxy 2	Antistatic
Sizing rate (%)	0.46	0.10	0.10	0.25	0.10	0.15	0.12–0.15
Density ($\times 10^{-9} \text{ t.mm}^{-3}$)	1.82	1.82	1.82	1.81	1.82	1.78	1.8
Breaking stress (N)	3,090	2,975	3,280	3,135	3,280	>2,700	3,400
Young modulus (MPa)	45,200	37,602	42,635	42,226	37,506	36,991	17,042
Number of fibers ($\times 10^3$)	50	50	50	50	50	12	50
Section width (mm)	8.0	10.0	9.0	9.0	9.0	3.5	19.0
Section height (mm)	1.0	1.0	1.0	1.0	1.0	0.6	1.0
Cohesion factor	3	0	0	1	0	2	0

characterization methods inspired by 3-point bending of homogeneous materials have been proposed.^{23–25}

However, the specimen remains fixed on one side, which potentially generates a cantilever effect, and the test only gives a stiffness at one deflection length. In addition, it has been shown that the bending behavior, whose stiffness is very low, is highly non-linear due to its multi-scale architecture and that it depends on time and loading history.^{18,21,26,27} It is therefore necessary to use other characterization techniques. The Kawabata Evaluation System (KES)²⁸ captures the moment-curvature curves under cyclic loading. However, this technique, which is viable for clothing textile, is not suitable for technical reinforcements, which are thicker and stiffer. Therefore, De Bilbao et al.¹⁵ proposed a technique based on the generalized cantilever, where the reinforcement bends under its own weight, at different overhang lengths, and the deflections are captured by optical means to evaluate the bending stiffness. This principle has been adapted for the case of prepregs by combining the test with a temperature-controlled environment.¹⁹ It should be noted that other techniques have also been developed for the bending characterization of reinforcements at the mesoscopic scale.^{26,29}

The principle of the bending tests chosen for this study is the Generalized Cantilever Test instrumented by optical measurements, developed by De Bilbao¹⁸ and shown in Figure 3. This test has been shown to be effective in studying the bending of textile structures as it enables different bending lengths to be studied, thus making it possible to consider the whole bending behavior. The textile structure is embedded on one side and left free on the other side to bend under its own weight. The test is carried out for different lengths of yarns and repeated several times (at least 10) to ensure reliable results.

The instrument has two main parts: mechanical and electronic. The mechanical part includes a rectangular support made of PVC (Polyvinyl chloride), on which a rectangular

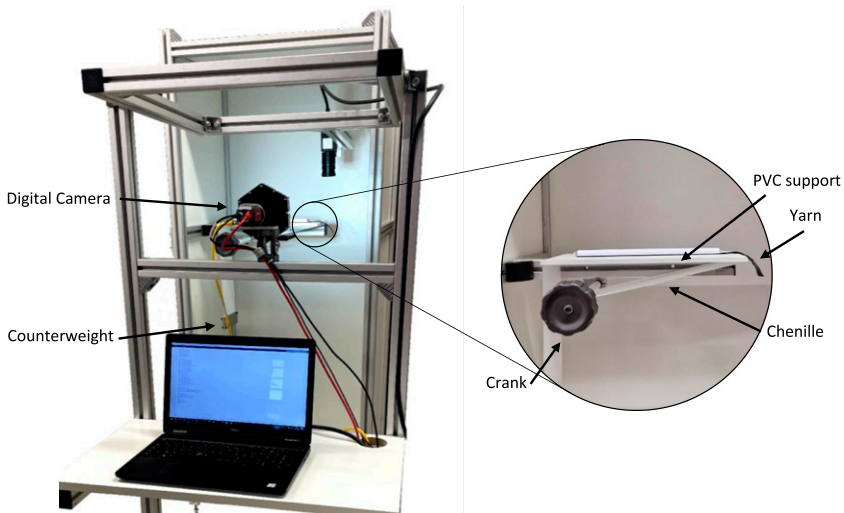


Figure 3. Bending device.

polymer chenille is placed and moved horizontally by a crank. A counterweight is attached to the other side of the chenille to stabilize it. Then, a yarn is laid gently on the chenille and a transparent plate is carefully placed on the yarn, at a variable height depending on the thickness of the yarn to avoid any pressure being applied on the yarn. The plate is just used to overcome the initial curvature of the yarn and to ensure full contact between it and the chenille. During the experiment, the chenille and the yarn displace horizontally at the same speed, without any relative sliding between them, and consequently, without any friction between the yarn and the chenille. The displacement of the yarn is ensured by the rotation of a crank and measured by a ruler which is fixed on the PVC support. When the yarn advances, it bends under its own weight. The yarn bending increases continuously when the overhang length increases. Images of the bending are captured by a CCD camera (Allied Vision Manta G504-B, 12 Mega Pixels) at different steps of displacement of the yarn. All the tests were performed with controlled and measured temperature (between 18°C and 25°C) and hygrometry (between 40% and 60%).

Results and discussion

Experimental characterization of the bending, consequences on the measurements, observations and first conclusions

The bending tests were initially analyzed for five overhang lengths: 70 mm, 90 mm, 100 mm, 120 mm and 150 mm. For each length, an image was captured by the digital camera. The image was then analyzed by a MATLAB program, developed in the Laboratory of Mechanics Gabriel Lamé, to reconstruct the bending profiles by scanning pixels of the image. With this program, three bending profiles were extracted and inverted: upper, lower and medium, as shown in Figure 4.

The three bending profiles are due to the twisting of the yarn during bending. The difference between the upper and lower profiles represents the amount of twisting during bending, whereas the medium profile represents the average of the upper and lower profiles. While this point is interesting, the analysis of this phenomenon is not the topic of the present publication and will be dealt with in a following study. As shown below, the sensitivity of the bending test means that this point can be neglected in the context of the present study.

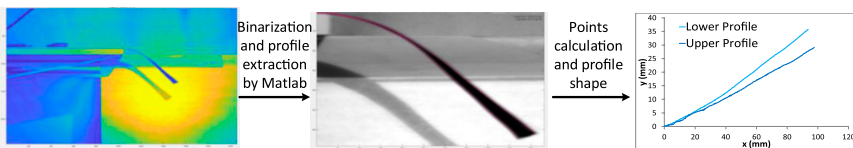


Figure 4. Bending profiles.

From a practical point of view, the upper profiles appear more robust for the post-processing and reconstruction; these profiles were therefore used for the rest of the study (Figure 5).

As the number of configurations was very high (7 batches, 10 tests per batch, 5 lengths per test), and a similar behavior was observed on all batches, the complete results for all batches at each length will not be presented. The analysis was done based on the complete results of a configuration and the comparison of different batches to a given test configuration. The results obtained for the upper profiles of batch B with a repeatability of 10 tests are presented on Figure 6 for all overhang lengths and the results for all the batches with a 150 mm overhang length are presented on Figure 7. The average deflection and the associated standard deviations are given in Table 2.

The first observation that can be made is the huge variability of the bending behavior for the same yarn or for each test configuration, regardless of the batch or the length, as can be clearly seen on Figures 6 and 7 and Table 2. This variability is even greater for batch F (Figure 6), which is due to several reasons, among which the fiber arrangement along the yarn, but the most important one is undoubtedly the heterogenous distribution of the sizing inside the yarns. Therefore, a minimum repeatability of 10 experiments, at least, seems to be necessary during this type of test to ensure a correct definition of the average bending behavior. Secondly, the medium curves of the upper profiles of all batches are presented on the same graph to illustrate the average bending trend of each batch, as shown in Figure 8. This enables comparison between the bending profiles of the different batches and shows that the bending profiles are, as expected, very different, even for yarns with a very similar constitution.

However, the bending stiffness of a sample depends not only on the material behavior and properties but also on the sample geometry (quadratic moment). In addition, the bending profile also depends on the loading, that is in the present case, imposed by the sample density, depending on the number, size and material of the fibers. In the present study, the yarns of batches A, B, C, D, E are of the same type and have the same section shapes. They will therefore be considered first and analyzed to evaluate the link between

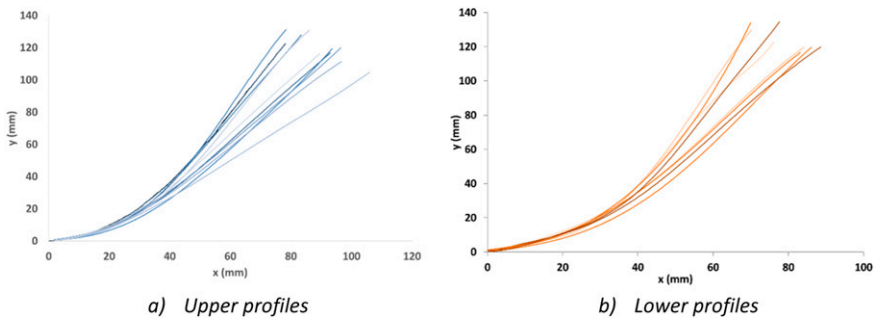


Figure 5. Profiles of 10 bending experiments of batch B, at an overhang length of 150 mm. (a) Upper profiles. (b) Lower profiles.

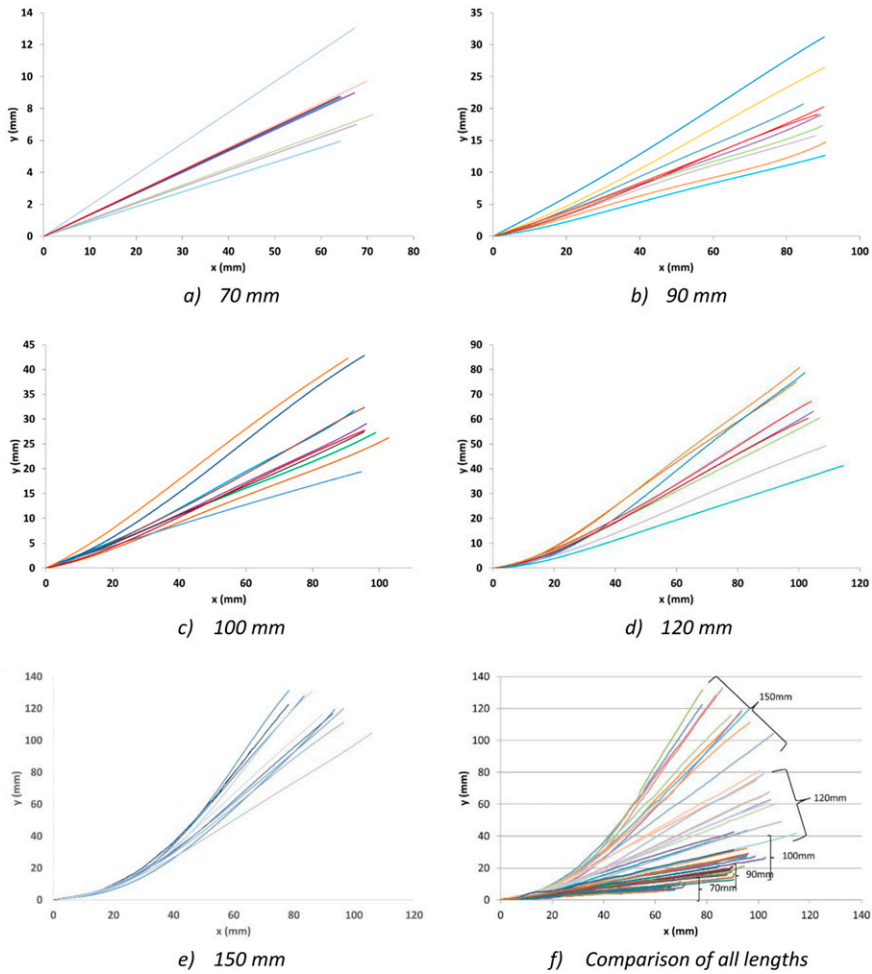


Figure 6. Profiles of different bending lengths of batch B. (a) 70 mm. (b) 90 mm. (c) 100 mm. (d) 120 mm. (e) 150 mm. (f) Comparison of all lengths.

cohesion and bending behavior. The other two batches will then be analyzed, using a different post-processing strategy.

Relation between bending profile and cohesion

Figure 9 presents a comparison between the bending stiffness of batches of the same type (A, B, C, D, E), at three selected overhang lengths. First, it can be seen that the bending test successfully discriminates the differences between different batches of the same nature. Some yarns have a stiffer behavior whatever the length (A) whereas others are more flexible (B and C). They can therefore be classified as follows: $C < B < D < A$. Batch

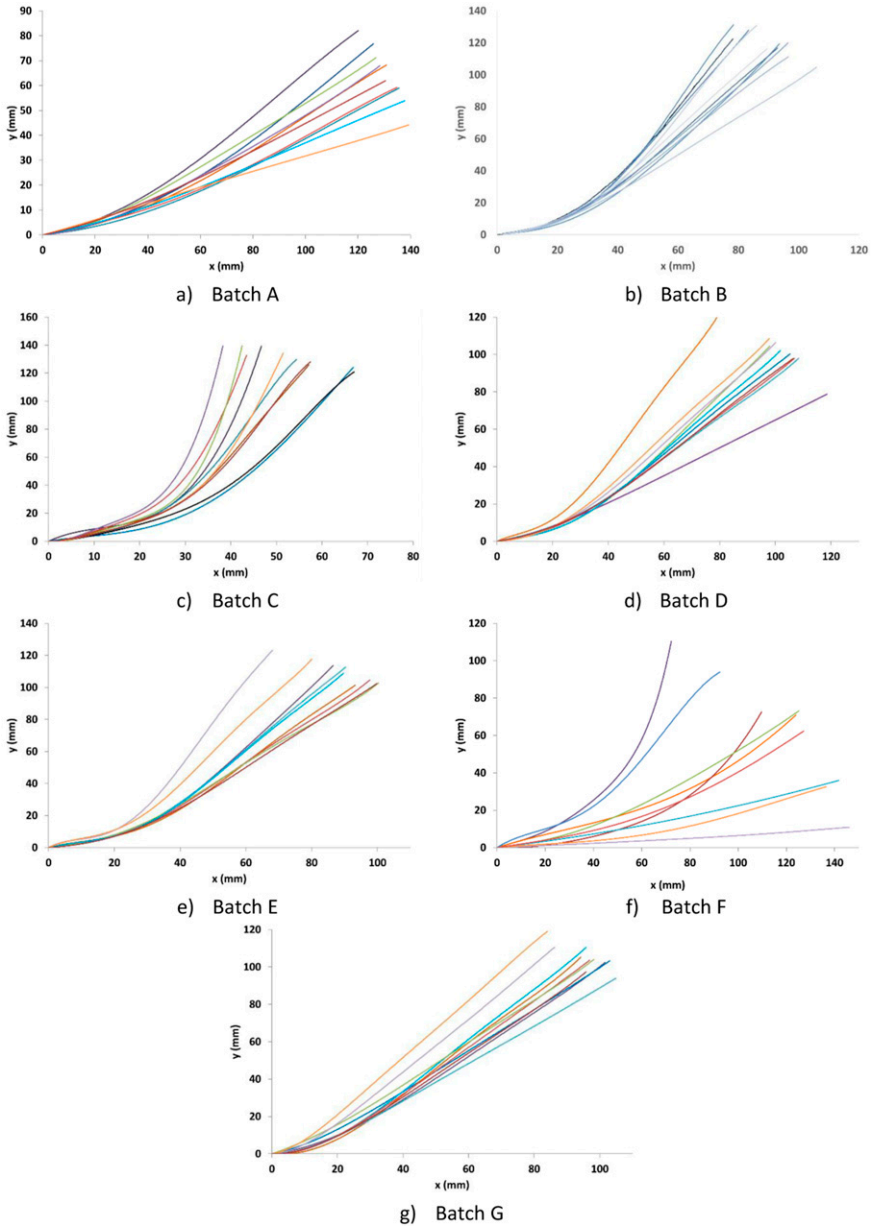
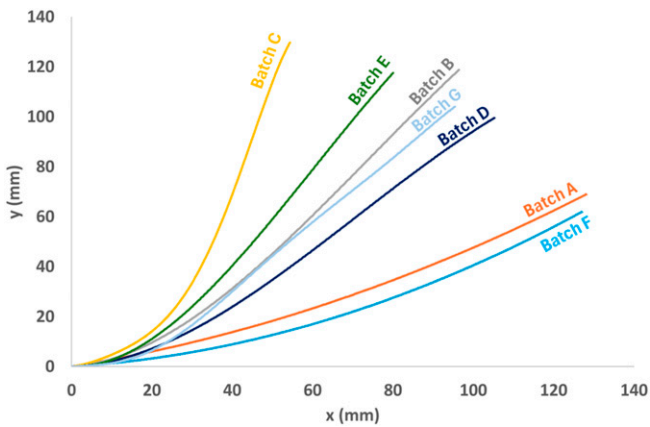


Figure 7. Bending profiles for each batch with a 150 mm bending length.(a) Batch A. (b) Batch B. (c) Batch C. (d) Batch D. (e) Batch E. (f) Batch F. (g) Batch G.

Table 2. Average deflection and standard deviations for each batch with 150 mm of bending length.

	Batch A	Batch B	Batch C	Batch D	Batch E	Batch F	Batch G
Average deflection (mm)	64.9	120.2	132.5	101.0	117.3	62.5	104.7
Standard deviation (mm)	10.8	8.35	7.1	10.6	9	31.0	7.0
Standard deviation (% of the average value)	17.2	6.9	5.4	10.5	7.7	49.6	6.7

**Figure 8.** Medium profiles for each batch with 150 mm of bending length.

E appears to be different, with a stiffer behavior for a low length and a rough relaxation. This can be explained by a heterogeneous distribution of cohesion along the yarn. However, when the high overhang lengths are taken into consideration, these results correspond to the initial classification of the yarns' processability, as presented in Table 1. Batch A does not bend easily under its own weight; its bending behavior is very stiff, which corresponds to a high cohesion factor and thus a low processability. On the contrary, batches B, C and E are more flexible for the same overhang length; their cohesion factor is low and thus they can be more easily processed. In between, batch D presents an average behavior and this batch also has an average cohesion factor and thus an average processability. Hence, it can be concluded that the sensitivity of the bending test is very good and that it can be directly used to distinguish the cohesion of yarns with an identical structure.

To conclude, variations in average bending stiffness on batches A, B, C, D, E can be clearly observed. Despite the intrinsic variability due to the yarns' structure, the average bending behaviors discriminate the cohesion of the different batches very clearly, enabling batches with very close sizing rates to be distinguished. The most interesting fact, however, is that the discrimination is very clear between batches with different

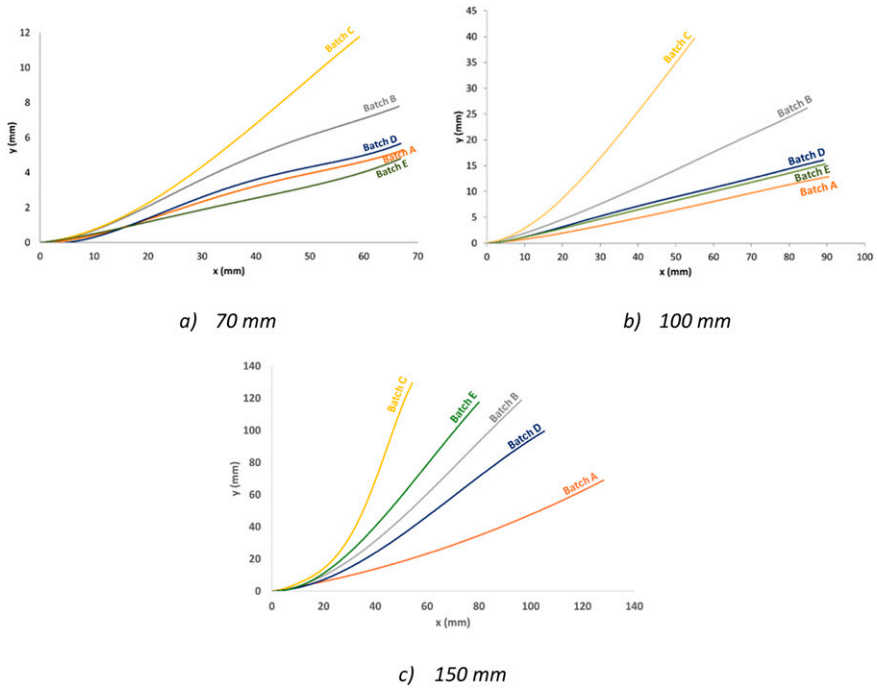


Figure 9. Comparison of medium curves of upper profiles for comparable batches at 3 different lengths. (a) 70 mm. (b) 100 mm. (c) 150 mm.

processabilities especially for high overhang lengths of bending. This confirms that the bending test is an excellent candidate to bring out the differences in yarn cohesion. Thus, for batches with identical structures, for example, a simple comparison of the profiles at a defined length before launching production, or upon material receipt, is sufficient to discriminate and/or qualify the batches in terms of cohesion and therefore their processability. The first objective outlined in the previous section (“Material and methods”), namely material incoming inspection, and part of the second one, that is making changes in sizing type without having to undertake a lengthy test campaign, have thus been attained. Concerning the third objective, that is comparing the cohesion of yarns with different structures and compositions, the high sensitivity of the relation between bending behavior and cohesion and processability is clearly evidenced, confirming the great potential of bending to characterize the cohesion of a fibrous fabric. Beyond processability, however, the test is able to discriminate very few sizing rate variations. This test could possibly be used to estimate the sizing rate to within an order of magnitude from the bending behavior.

As previously mentioned, the comparison of overhanging length and profiles is not an intrinsic measure of the material as it depends on the yarn geometry. Thus, it is necessary to consider another post-treatment of this test to be able to discriminate and compare the

cohesion of yarn batches with different structures (density, geometry, etc.). The next section proposes a first approach.

Comparison of yarns with different structures

While the previous strategy, based on comparing profiles, is very efficient, it does not enable batches A, B, C, D, E to be compared with batches F and G because the dimensions and the structures are different. These structural differences, given in Table 1, are illustrated on Figure 10. Thus, it is necessary to define a bending equivalent stiffness intrinsic to the fibrous structure and independent of yarn dimensions. This problem is inherently complex because of the heterogeneous nature of the yarn; hence, the definition of bending stiffness in terms of homogeneous material is ill-adapted.

Some authors focused on modeling the bending behavior, integrating enriched physics and cinematics in the model (Cosserat, 2nd gradient^{30–32}). The objective of the present study is not to solve the problem of the definition of a behavior law or of bending behavior parameters, but rather to determine a reachable strategy which can be quickly implemented, especially in an industrial context. The strong sensitivity of the bending/cohesion relation, combined with the high variability obtained on the bending behavior, means that an approximate strategy based on homogeneous continuum mechanics can be considered. To achieve this, the notion of cohesion must be defined as the ability of the fibers to move relative to each other. During bending, this sliding can be expressed in the longitudinal direction and, considering homogeneous continuum mechanics, by the shear stiffness G_{13} . This is well illustrated by the angular orientation of the section presented in Figure 1.

Considering the overhanging length, which is an important element of the discrimination, it seems possible to reproduce the yarn bending behavior approximately driven by the shear coefficient with an infinite strain calculation and an anisotropic material. Moreover, comparing the bending profiles in order to classify the bending stiffness of yarns is not always easy because the distribution of the sizing along the yarns is not always homogenous. Thus, some bending profiles appear to be more rigid at the beginning of bending and suddenly become less rigid after a defined overhang length of bending. The

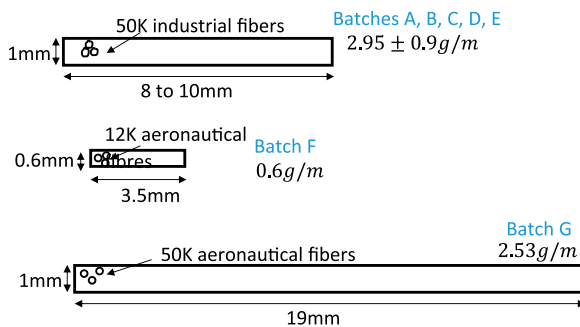


Figure 10. Yarns structure.

main difficulty with this experiment remains its inability to compare the bending profiles of yarns of different natures in order to classify their cohesion. Therefore, another intrinsic parameter needs to be defined to accomplish the comparison correctly.

Finite element simulations of the bending test

Usually, yarns have a heterogenous structure, in which the bending stiffness is related to two main physical parameters: the longitudinal modulus of fibers and their capacity to displace in the longitudinal direction during bending. This displacement represents the shear occurring during bending, which is related to the shear modulus of the yarns.

In this study, in a first approach, we considered the yarns as a homogenous orthogonal equivalent material. Under this assumption, the ability of yarns to be sheared during bending is directly related to the shear modulus G_{13} (the 1 refers to the longitudinal direction of the yarn). Nevertheless, this approach does not consider the internal crimping of the fibers that constitute the yarn. Therefore, the simulation cannot accurately reproduce the real bending profiles as they are observed experimentally. For more accurate simulations, another theoretical approach, using a micro-polar structure, could be used. However, setting up this approach requires more investment and is therefore more difficult to implement in an industrial context. The use of G_{13} nevertheless makes it possible to reproduce numerical profiles of bending close to the experimental ones, at certain overhang lengths. With the identified G_{13} using this inverse approach, the sought-after medium bending profile can be defined and used to compare the bending stiffness of different batches. Using this approach, finite element simulations were performed by Abaqus® software, with C3D20 elements, as shown in Figure 11.

Thanks to these simulations, numerical curves were obtained by identification of G_{13} and compared with the experimental profiles. The numerical curves are relatively close to the experimental ones, as shown in Figure 12. Depending on the batches, however, they reproduce the curvature more or less well; this illustrates the limit of a homogeneous approach with very variable results. Nevertheless, in a first approach, this method is a very simple and efficient way to compare the G_{13} values of different batches, which could be used as an indicator of the bending stiffness of these batches.

The values of G_{13} of each of the seven tested batches were computed from the simulations, and are presented in Table 3:

With these values, the bending rigidity of the batches can be classified as follows:



Figure 11. Modeling of yarn by a homogeneous transverse isotropic material.

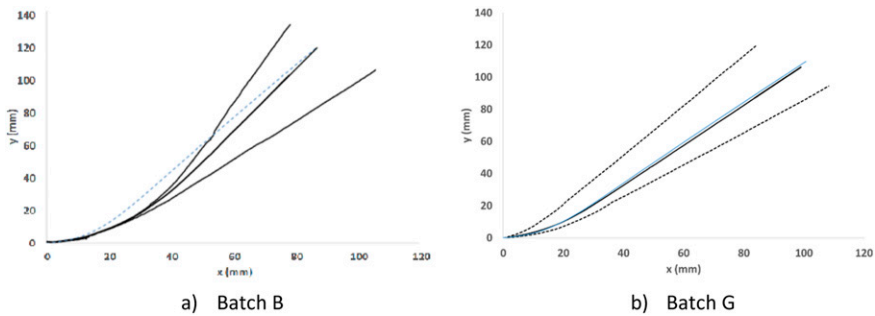


Figure 12. Comparison between numerical (blue dotted line) and experimental (maximum, minimum, and medium) curves (black lines) of bending for batches B and G. (a) Batch B. (b) Batch G.

Table 3. Modulus G_{13} identified by finite element simulations.

	Batch A	Batch B	Batch C	Batch D	Batch E	Batch F	Batch G
Longitudinal shear Modulus G_{13} (10^{-2} MPa)	6.32	2.47	1.65	3.85	2.75	12.37	1.37
Cohesion factor	3	0	0	1	0	2	0

$$G_{13_F} \gg G_{13_A} \gg G_{13_D} > G_{13_E} > G_{13_B} > G_{13_C} > G_{13_G}$$

Globally, the shear modulus is able to reproduce the resetting of the processability, at least by group: a high shear modulus and low processability for batches A and F, average modulus and processability for batch D, and low modulus with high processability for batches B, C, E and G. However, perhaps due to the approximate calculation of the shear modulus performed for the moment, it is still difficult to discriminate batches within a group. Although the resetting is approximate, this method can correctly discriminate small deviations of cohesion, with a difference of 48% between batches D and A, 40% between batch D and batch B and 33% between batch D and E. Remember that batches A, B, and D have globally the same material characteristics and that their differences lie in the type and sizing rate as well as the processability. Nevertheless, to analyze the relevance of this method, batches F and G must be analyzed because their structure and dimensions are very different, which justified the definition and use of a mechanical parameter.

The main problem with batch F is that the bending profile results are widely scattered, much more so than for the other batches (Figure 7). It is thus unreliable to consider the average curve. Moreover, batches F and G show a different bending behavior from the other batches (Figure 7). The bending behavior of fibrous networks has generally a high and relatively clear non-linearity whose variability can lead to very different profiles. This phenomenon can be seen on Figure 9. Comparing the average curves of batch E for

different overhanging lengths, one can see that batch E presents a low overhanging length until 100 mm and then a high overhanging length at 150 mm. As has already been studied with the shear,¹⁵ it seems that two types of cohesion can be distinguished: a static cohesion, driven by sticking during which the longitudinal sliding between fibers is low, and a dynamic cohesion, driven by the residual friction during the fibers' longitudinal sliding. Thus, higher quality yarns, that is, more regular and smoother, have a lower residual friction and therefore a higher non-linearity. It is fundamental to explore even further, in the future, the relation between bending and cohesion, and to highlight the different physical phenomena related to cohesion in order to better understand and analyze this phenomenon.

Lastly, this strategy, although approximate, makes it possible to compare batches with different structures and to highlight, with a simple test and inverse identification calculation, the behavior variability during the process; this was the third goal of this study. It is thus possible to define and measure a yarn cohesion indicator, whatever the structure and constitution of the yarn. Hence, beyond its efficiency in material incoming inspection, this strategy can be used to study, for example, a change or an evolution of the raw material used for the process. There currently remains a limit however: the post-treatment specific to the constitutive material is still difficult to address if we wish to remain within relatively simple physics.

Conclusion

Although yarn cohesion is of great importance for various manufacturing processes, there is currently no efficient strategy to evaluate this property upstream of the process. This paper has therefore focused on the evaluation of the cohesion of carbon fiber yarns using bending tests, assessing the global cohesion of yarns by means of their bending rigidity.

The results highlight that when the yarns are of the same nature, they can be very efficiently classified according to their cohesion by comparing their bending profiles. It concerns yarns A, B, C and D, which can be classified as follow, from the more rigid (and thus with higher cohesion and lower processability) to the less one: $A > D > B > C$. It can be confirmed that the sizing rate significantly influences the bending rigidity and thus the cohesion: the lower the sizing rate, the greater the fiber mobility and thus the lower the cohesion. Therefore, the proposed strategy enables to distinguish between the best batches as regards processability, that is batches B and C, the intermediate batch D and the worse batch A. The case of batch E was very interesting as it demonstrates the influence of the heterogeneity of sizing distribution. However, for high overhang lengths, the results correspond to the initial classification of the yarns' processability presented in [Table 1](#). Moreover, a very interesting point concerning the bending test is that it is very sensitive to cohesion variation, that is to say it is able to clearly discriminate batches with very similar and low sizing rates as regards their processability. All these points confirm that the bending test is an excellent candidate to bring out the differences in yarn cohesion and can be easily used in an industrial context for yarns of the same nature. It could, for instance, be used as a very efficient material incoming inspection tool. For yarns of different natures, even if this point remains a challenge, the bending rigidity was evaluated

relatively efficiently by the shear modulus of an equivalent transverse isotropic homogeneous material (G_{13}). Thus, the targeted classification of all the yarns, whatever their structure and constitution, with regard to their processability has been achieved using the proposed strategy. Even if the definition of an intrinsic indicator remains difficult, the strategy also confirms that bending behavior is undoubtedly the best candidate to analyze this phenomenon and enables to distinguish the three main groups as regards the processability: the best batches (B, C, E and G) the intermediate batch (D) and the worse batches (A and F). Beyond the classification of the batches as a function of their processability, which was the main goal of this study, the bending test confirms the strong and very sensitive correlation between the bending behavior of the yarns and their cohesion, and thus its significant potential to study cohesion. The richness of the results obtained, that is, a spectrum of bending profiles with different lengths, for different batches with different structures, opens up an important field of analysis which remains to be carried out. Observing more precisely the bending responses, it is possible to highlight specific aspects linked to the yarns' cohesion and behavior. This will be the subject of another study, but some initial conclusions can already be drawn. First, the existence of two steps in cohesion seems to be confirmed and may be the reason for the non-linearity of the bending behavior of yarns. The first step, which can be considered as static cohesion, is driven by the sticking of numerous fibers together, while the second one, which can be considered as dynamic cohesion, is driven by the sliding resistance between the fibers. In addition, the study has also revealed the influence of the heterogenous distribution of the sizing along the yarn, inducing a strong dispersion of the bending results. From an industrial point of view, the method applied here is very simple and efficient but, to go further in the understanding of the relationship between bending and cohesion, and the physical phenomena involved during the bending behavior of the batches, considerable work remains to be done. Moreover, the cohesion of yarns is a highly complicated phenomenon and one way to better understand this phenomenon might be to evaluate global cohesion by comparing different tests such as bending but also shear and friction.

Declaration of conflicting interests

The author(s) declared no potential conflicts of interest with respect to the research, authorship, and/or publication of this article.

Funding

The author(s) received no financial support for the research, authorship, and/or publication of this article.

ORCID iDs

Audrey Hivet  <https://orcid.org/0000-0003-0067-7575>

Anwar Shanwan  <https://orcid.org/0000-0002-3441-3829>

Samir Allaoui  <https://orcid.org/0000-0001-9673-1016>

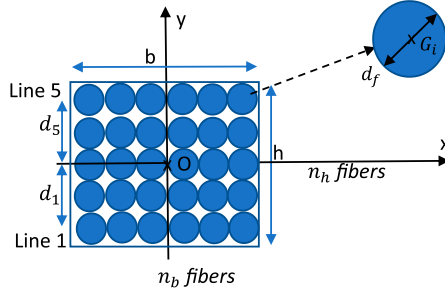
References

1. Salem MM, De Luycker E, Delbe K, et al. Experimental investigation of vegetal and synthetic fabrics cohesion in order to prevent the tow sliding defect via frictional and pull-out test. *Compos Appl Sci Manuf* 2020; 139: 106083.
2. Valizadeh M, Ravandi SA, Salimi M, et al. Determination of internal mechanical characteristics of woven fabrics using the force-balance analysis of yarn pullout test. *The Textile Institute* 2008; 99: 47–55.
3. Bai R, Li W, Lei Z, et al. Experimental study of yarn friction slip and fabric shear deformation in yarn pull-out test. *Compos Appl Sci Manuf* 2018; 107: 529–535.
4. Steinke K and Sodano H. Improved inter-yarn friction and ballistic impact performance of zinc oxide nanowire coated ultra-high molecular weight polyethylene (UHMWPE). *Polymer* 2021; 231: 124125.
5. Hajsadeghi M, Chin CS and Jones SW. Development of a generic three-dimensional finite element fibre pullout model. *Construct Build Mater* 2018; 185: 354–368.
6. Nilakantan G and Gillespie JW. Yarn pull-out behavior of plain woven Kevlar fabrics: effect of yarn sizing, pullout rate, and fabric pre-tension. *Compos Struct* 2013; 101: 215–224.
7. Nilakantan G, Merrill R, Keefe M, et al. Experimental investigation of the role of frictional yarn pull-out and windowing on the probabilistic impact response of kevlar fabrics. *Compos B Eng* 2015; 68: 215–229.
8. Teklal F, Djebbar A, Allaoui S, et al. A review of analytical models to describe pull-out behavior—fiber/matrix adhesion. *Compos Struct* 2018; 201(4): ■■■.
9. Latil P, Orgeas L, Dumont P, et al. Mechanics of a fibre bundle during bending: an analysis using X-ray microtomography. In: 9th Euro Solid Mech Conf, Madrid, Spain, July 2015, pp. 1–2. Euromech.
10. Latil P, Orgeas L, Geindreau C, et al. Towards the 3D in situ characterisation of deformation micro-mechanisms within a compressed bundle of fibres. *Compos Sci Technol* 2011; 71(4): 480–488.
11. Barella A and Sust A. Cohesion phenomena in rovings and yarns: part IV: cohesion of twisted rovings, its effect on yarn properties. *Textil Res J* 1965; 35(6): 491–496.
12. Barella A and Sust A. Cohesion phenomena in cotton rovings and yarns: part II: influence of twist on yarn cohesion. *Textil Res J* 1963; 33(1): 75–79.
13. Gokarneshan N, Ghosh A, Anbumani N, et al. Investigation of inter fiber cohesion in yarns. I. Influence of certain spinning parameters on the cohesion in cotton yarns. *Fibers Polym* 2005; 6(4): 336–338.
14. Rubino M, Wielhorski Y and Roux S. Transverse compaction of twisted carbon yarns: experiment and elasto-plastic Mohr–Coulomb modeling. *Compos Part A Appl Sci and Manufac* 2024; 176: 107873.
15. Wendling-Hivet A, Ferré MR, Allaoui S, et al. Study of the cohesion of carbon fiber yarns: in-plane shear behavior. *Int J Material Form* 2017; 10(5): 671–683.
16. Peirce FT. 26—the “handle” of cloth as a measurable quantity. *J of the Tex Institute Trans* 1930; 21(9): T377–T416.

17. Poppe C, Rosenkranz T, Dörr D, et al. Comparative experimental and numerical analysis of bending behaviour of dry and low viscous infiltrated woven fabrics. *Compos Appl Sci Manuf* 2019; 124: 105466.
18. De Bilbao E, Soulat D, Hivet G, et al. Experimental study of bending behaviour of reinforcements. *Exp Mech* 2010; 50(3): 333–351.
19. Cornelissen B and Akkerman R. Analysis of yarn bending behaviour. *IEEE (Inst Electr Electron Eng) Trans Biomed Eng*. 2009.
20. Soteropoulos D, Fetfatsidis K, Sherwood J, et al. Digital method of analyzing the bending stiffness of non-crimp fabrics. *AIP Conf Proc* 2011; 1353: 913–917.
21. Alshahrani H and Hojjati M. Bending behavior of multilayered textile composite preregs: experiment and finite element modeling. *Mater Des* 2017; 124: 211–224.
22. Dangora L, Mitchell C, White K, et al. Characterization of temperature-dependent tensile and flexural rigidities of a cross-ply thermoplastic lamina with implementation into a forming model. *Int J Material Form* 2018; 11: 43–52.
23. Wang J, Long A and Clifford M. Experimental measurement and predictive modelling of bending behaviour for viscous unidirectional composite materials. *Int J Material Form* 2010; 3: 1253–1266.
24. Mathieu S, Hamila N, Bouillon F, et al. Enhanced modeling of 3D composite preform deformations taking into account local fiber bending stiffness. *Compos Sci Technol* 2015; 117: 322–333.
25. Wang Y, Li X, Xie J, et al. Numerical and experimental investigation on bending behavior for high-performance fiber yarns considering probability distribution of fiber strength. *Textiles* 2023; 3: 129–141.
26. Sourki R, Crawford B, Vaziri R, et al. Meso-level bending/reverse-bending analysis of dry woven fabrics: observing an irreversible behavior during forming. *Compos Struct* 2022; 282: 115124.
27. Boisse P, Colmars J, Hamila N, et al. Bending and wrinkling of composite fiber preforms and preregs. A review and new developments in the draping simulations. *Compos B Eng* 2018; 141: 234–249.
28. Kawabata S. *The standardization and analysis of hand evaluation*. 2nd ed. Osaka, Japan: Textile Machinery Society of Japan, 1980.
29. Margossian A, Bel S and Hinterhoelzl R. Bending characterisation of a molten unidirectional carbon fibre reinforced thermoplastic composite using a dynamic mechanical analysis system. *Compos Appl Sci Manuf* 2015; 77: 154–163.
30. De Luycker E and Hamila N. Modeling of hyperelastic bending of fibrous media using second-gradient isogeometric analysis: weaving and braiding applications. *Compos Appl Sci Manuf* 2023; 167: 107415.
31. Madeo A, dell'isola F, Ianiro N, et al. A variational deduction of second gradient poroelasticity II: an application to the consolidation problem. *J Mech Mater Struct* 2008; 3: 607–625.
32. Forest S and Sab K. Cosserat overall modeling of heterogeneous materials. *Mech Res Commun* 1998; 25(4): 449–454.

Appendix

Appendix I



Let's consider a simple rectangular assembly with an odd number of lines of n fibers, all identical, with a width b and a height h :

- $h = n_b d_f$; $n_h = 2k_h + 1$
- $b = n_b d_f$
- $n = n_b n_f$

The yarn comprises $2k_h + 1$ lines of n_b fibers with a circular section:

$$I_{G_{ix}}(f_i) = \frac{\pi d_f^4}{64}$$

$$I_{Ox}(\text{yarn}) = \sum_{i=1}^n I_{Ox}(f_i)$$

If y_i is the distance between the (G_i, \mathbf{x}) axis and the (O, \mathbf{x}) axis and according to Huyghens' theorem:

$$I_{Ox}(f_i) = I_{G_{ix}}(f_i) + S_f \times y_i^2$$

$$I_{Ox}(\text{yarn}) = \sum_{i=1}^n (I_{G_{ix}}(f_i) + S_{f_i} \times y_i^2)$$

As all fibers are identical:

$$I_{Ox}(\text{yarn}) = \sum_{i=1}^n \left(\frac{\pi d_f^4}{64} + \frac{\pi d_f^2}{4} \times y_i^2 \right)$$

$$I_{Ox}(yarn) = \frac{n\pi d_f^4}{64} + \frac{\pi d_f^2}{4} \sum_{i=1}^n y_i^2$$

Let j be a particular line of fibers; the y_j distance is the same for all the fibers of the line j and then:

$$y_j^2 = d_f^2(k_h + 1 - j)^2$$

$$I_{Ox}(yarn) = \frac{n\pi d_f^4}{64} + \frac{\pi d_f^2}{4} \sum_{i=1}^{n_b} \sum_{j=1}^{n_h} d_f^2(k_h + 1 - j)^2$$

$$I_{Ox}(yarn) = \frac{n\pi d_f^4}{64} + \frac{\pi d_f^2}{4} n_b d_f^2 \sum_{j=1}^{n_h} (k_h + 1 - j)^2$$

After calculating:

$$I_{Ox}(yarn) = \frac{n\pi d_f^4}{64} + \frac{\pi d_f^4}{12} n_b k_h (k_h + 1)(2k_h + 1)$$

Finally:

$$\frac{I_{Ox}(ya)}{I_{Gix}(f_i)} = n + \frac{16}{3} n_b k_h (k_h + 1)(2k_h + 1)$$